Amplitude Dependency of Damping in Buildings and Estimation Techniques

Yukio Tamura

Director, Wind Engineering Research Center, Tokyo Polytechnic University, 243-0297, Japan
yukio@arch.t-kougei.ac.jp

ABSTRACT:

This paper first discusses the dynamic properties of buildings, especially amplitude dependency of damping ratio. It is emphasized that there is no evidence of increasing damping ratio in the very high amplitude range within the elastic range of main frames, unless there is damage to secondary members or architectural finishing. The damping ratio rather decreases with amplitude from a certain tip drift ratio defined as "critical tip drift ratio". Then, damping predictors based on a recent damping database are introduced, and design values for damping ratio are recommended. Next, the feasibility and efficiency of two simple and user-friendly but accurate damping estimation techniques are discussed. One is the Frequency Domain Decomposition technique, which uses Singular Value Decomposition of the Power Spectral Density matrix of multiple outputs, and the other is the Multi-mode Random Decrement technique. Both can be applied to ambient excitations such as micro-tremors, enabling easy handling of closely-spaced and even repeated modes. Some full-scale examples demonstrating the damping estimation efficiency of both techniques are also shown.

INTRODUCTION

In order to evaluate the responses of buildings, their dynamic characteristics such as natural frequencies, mode shapes and damping ratios should be accurately known. It is well known that a structure can be damped by mechanisms with different internal and external characteristics: friction between atomic/molecular or different parts, impacts, air/fluid resistance, and so on. Combination of different phenomena results in various types of damping. Vibration energy is finally dissipated as thermal energy, or is radiated outside the boundary of the system. Damping in buildings can not only reduce wind- or earthquake-induced vibrations, but also increase the onset velocity for aeroelastic instability. Generally, their mathematical descriptions are quite complicated, and not suitable for vibration analysis of complicated structures. In structural dynamics, damping is described by viscous, hysteretic, coulomb or velocity-squared models. Viscous damping occurs when the damping force is proportional to the velocity, and is mathematically convenient because it results in a linear second order differential equation for engineering structures. Transient decay of a viscously under-damped system is exponential. Fortunately, damping in buildings can be approximated by the viscous damping formula, even if there is no viscous material in it.

As there is no theoretical method for estimating damping in buildings, it should be estimated from full-scale data, which shows significant dispersion. Damping is the most important but most uncertain parameter affecting the dynamic responses of buildings. This uncertainty significantly reduces the reliability of structural design for dynamic effects. The causes of dispersion of full-scale damping are differences in structural materials, soil and foundations, architectural finishing, joint types, and vibration amplitude.

PHYSICAL CAUSES OF DAMPING IN BUILDINGS

There are various physical causes of damping in buildings, such as internal friction, plasticity, internal viscosity, external friction, radiation, external viscosity, aerodynamics, and so on. The majority of total damping of general buildings without any damping devices is radiation damping due to soil-structure interaction (SSI) and external friction damping (EFD) due to the friction between contact surfaces of elements such as frames, secondary members and architectural finishing.

AMPLITUDE DEPENDENCY OF DAMPING RATIO

General Tendency

The most realistic model of the physical EFD mechanism for built-up structures was evolved by Wyatt (1977) expressed by the "STICTION" term, which is randomly distributed with respect to amplitude. STICTION represents a STuck frICTION element, in which a contact surface between members does not move in the very low amplitude range, but begins to slip at a particular amplitude, thus losing its stiffness (Jeary, 1986) as illustrated in Fig.1. Figure 2 shows a typical amplitude dependency of dynamic properties obtained by the Random Decrement (RD) technique. The number of slipping contact surfaces increases with amplitude, so the damping ratio due to friction damping increases as the natural frequency decreases, as shown in Fig.2(a). This is expressed by the term "Stick-Slip" in Davenport & Hill-Carroll (1986). The integrated effect of a lot of different friction damping elements causes the building to respond as if it had a linear viscous damping system. Therefore, from a practical point of view, equivalent viscous damping, which models the overall damped behaviour of a structural system as being viscous, is often adopted in structural dynamics and is thought to be appropriate.

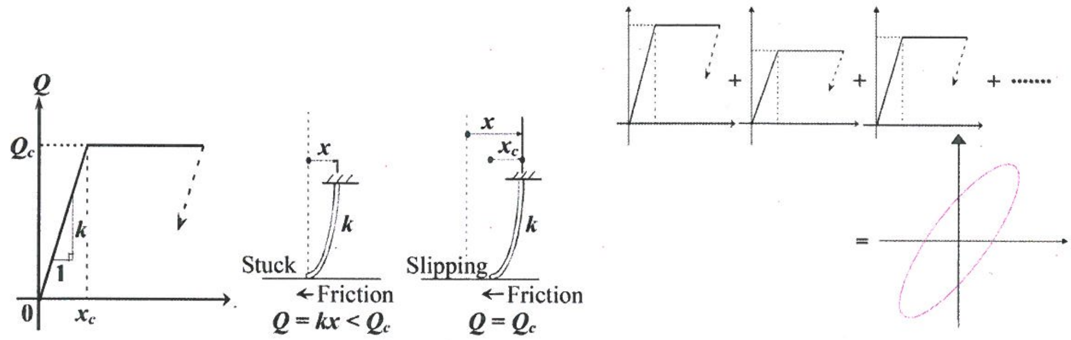

Figure 1 Stick-slip model for damping in buildings and viscous damping model

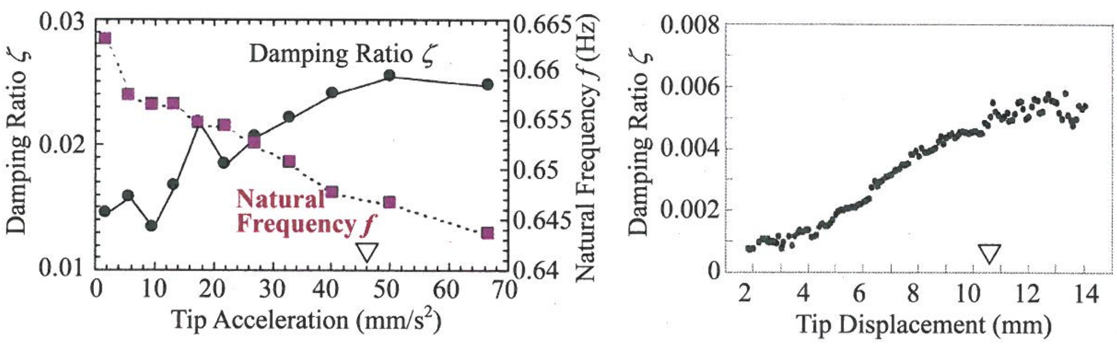

(a) 99m-high steel observatory building (Tamura et al., 2000) (b) 100m-high steel building (Jeary, 1998)

Figure 2 Amplitude dependency of dynamic properties of buildings obtained by RD technique

Critical Tip Drift Ratio

The variation of damping ratio with amplitude shown in Fig.2(b) suggests the following three parts: a low-amplitude plateau; a mid-amplitude slope; and a high-amplitude plateau (Jeary, 1998). It should be noted that the mid-amplitude slope where the damping ratio increases with amplitude ends at a relatively small amplitude level around 11mm in terms of the tip displacement, x_H. As the building height H is 100m, the tip drift ratio x_H/H is only 10^{-4}. Figure 2(a) also shows the same tendency, where the abscissa indicates the tip acceleration amplitude. The increasing tendency ends at around a_H = 46mm/s^2. Considering the natural frequency $f_1 = 0.66$Hz, the tip displacement x_H is roughly estimated by $a_H/(2\pi f_1)^2$ at 3mm. Thus, the tip drift ratio x_H/H is only 3×10^{-5} and still very small. Here, these tip drift ratios where the damping increasing tendency ends is defined as "critical tip drift ratio" in this paper. It should also be noted that the damping ratio at the high-amplitude plateau seems to begin to decrease at a higher amplitude region in Fig.2(a). The damping ratio does not increase any more with amplitude in the amplitude range above the critical tip drift ratio.

Figure 3 shows the results obtained from a Free Decay Damped Response (FDDR) after a sudden stop of excitation by a Hybrid Mass Damper (HMD) installed at the top of a 200m-high office building whose fundamental natural frequency f_1 = 0.26Hz. The variation of damping ratio is shown in Fig.3(b), where the abscissa indicates the tip velocity amplitude. It is obvious that the damping ratio increases in the low amplitude regime, and reaches its maximum around v_H = 6mm/s. Thus, the tip displacement $x_H \approx v_H/(2\pi f_1)$ is roughly estimated as 4mm. The critical tip drift ratio is estimated at $x_H/H = 2\times10^{-5}$, and is also very small. In the higher amplitude regime greater than this critical drift ratio, the damping ratio clearly decreases with amplitude.

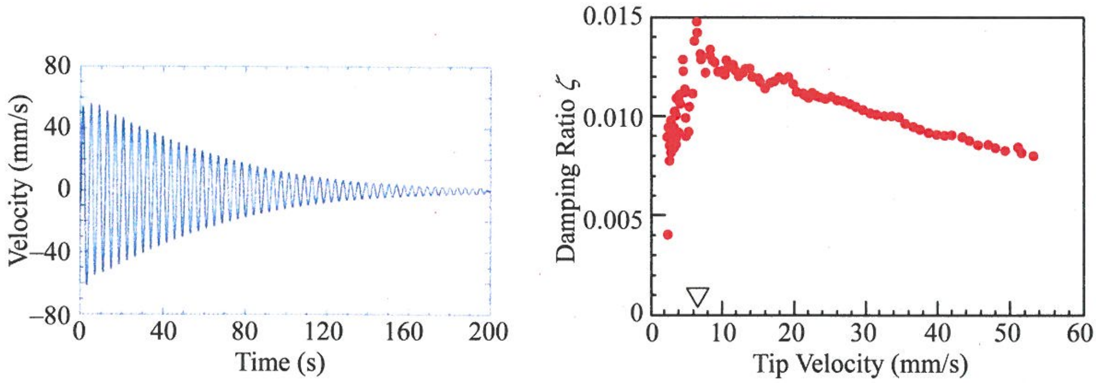

(a) FDDR (b) Variation of damping ratio with vibration level

Figure 3 Damping ratio obtained by FDDR of 200m-high office building (Okada et al., 1993)

The reason for the decrease in damping is decribed as follows. As already mentioned, increasing amplitude increases the number of slipping contact surfaces, and the damping ratio increases with amplitude. However, after reaching an amplitude level where all contact surfaces slip, the total friction force at the slipping contact surfaces causing friction damping does not increase any more with amplitude, i.e., the total friction force remains constant with increasing amplitude. For a simple forced vibration system with a constant damping force F, i.e. Coulomb damping, a steady state amplitude A and a circular natural frequency ω, the equivalent viscous damping coefficient C can be simply expressed as:

$$C = \frac{4F}{\pi A \omega} \tag{1}$$

The equivalent damping ratio ζ is given as:

$$\zeta = \frac{C}{2M\omega_0} = \frac{2F}{\pi AM\omega\omega_0} \tag{2}$$

Thus, if the friction damping force F is constant, the "damping ratio" decreases with increasing amplitude A. Figure 3(b) clearly shows the decreasing tendency with amplitude in the higher amplitude regime.

There has been a misunderstanding that the damping ratio increases with amplitude. However, that is not correct. It decreases with amplitude from the "critical tip drift ratio", which is very small, being in the order of 10^{-5} - 10^{-4}.

Damping Ratio at Very High Amplitude Level

There is not enough data on damping ratio at a very high amplitude level, and it is difficult to show general characteristics of dynamic properties in a very high amplitude regime. However, an example of dynamic characteristics in a very high amplitude level is shown in Fig.4 (Fukuwa et al., 1996), in which tendencies similar to Fig.2(a) are recognized in the natural frequency and damping ratio. The building is a three-story steel-framed experimental house with autoclaved lightweight concrete (ALC) panel slabs, ALC panel exterior walls, and plaster board partitions. The ALC panel exterior walls, with a thickness of 100mm, do not provide shear stiffness under horizontal loads. They are connected to the frames at their top only to permit a rocking type movement, although silicone sealing compounds fill the gaps between panels. This exterior wall system contributes significantly to structural damping, so it cannot be said that the results demonstrate the typical dynamic characteristics of general buildings. As the building height is only about 10m, the effect of SSI is very significant. Additionally, excitation was made up to 4×10^{-3} in terms of the tip drift ratio, and the maximum acceleration was almost 1,000milli-g. The maximum amplitude was large enough to damage the plaster board partitions, and cracks appeared not only in the ALC slabs but also in the ALC exterior walls.

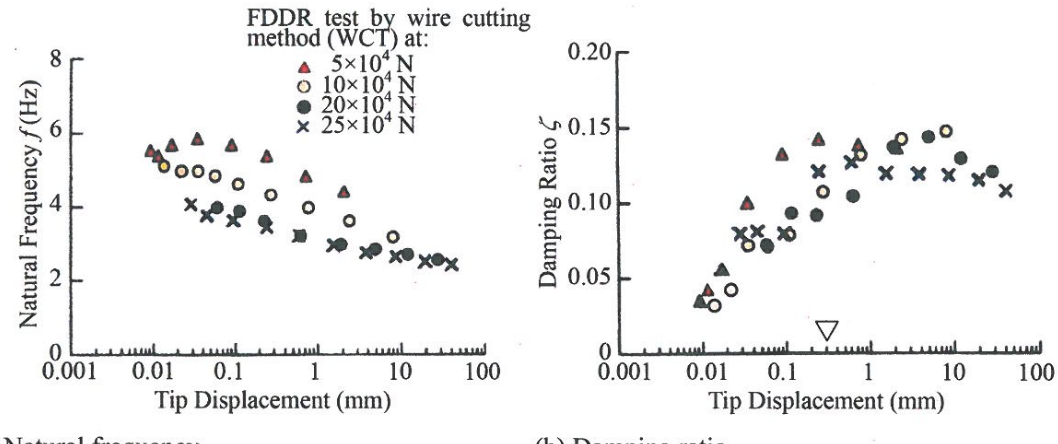

(a) Natural frequency (b) Damping ratio

Figure 4 Variations of dynamic properties of 3-story building with amplitude (Fukuwa et al., 1996)

Under the above conditions, the estimated damping ratio was large. However, it reached a maximum value at around 0.3mm tip displacement. Thus, the "critical tip drift ratio" is estimated at 3×10^{-5}, which is consistent with the previous results in Figs.2(a) and 2(b). Even after the damping ratio reached its maximum value with increasing amplitude, the natural frequency still decreased, as shown in

Figs.2(a) and 4(a). This is also reasonable, because the damping ratio can decrease even when the number of slipping contact surfaces increases, thus reducing the stiffness, if the increasing rate of amplitude is more significant than that of the number of slipping contact surfaces.

Here, it should be noted that the damping ratio never increases in a higher amplitude regime exceeding the "critical tip drift ratio" unless there is no additional source of damping forces. As explained above, there is a possibility of damage to secondary members such as non-load-bearing walls, interior partitions, slabs, and architectural finishing in the large amplitude range. However, if those kinds of damage are not allowed in allowable-stress-level design as in many current codes, a high damping ratio cannot be expected even near the elastic limit of frames. Considering the decreasing tendency shown in Fig.3(b), it is assumed that the maximum level damping ratio in Fig.4(b) is maintained because of the non-linear effect of SSI of a low-rise building and damage to partitions, non-load bearing ALC exterior walls and ALC slabs observed at a high amplitude level such as 1G acceleration response, while the main frames remained within elastic limit.

DAMPING DATABASE AND DESIGN VALUE RECOMMENDATIONS

Damping data have been collected by several researchers, e.g. Haviland (1976), Jeary (1986), Davenport & Hill-Carroll (1986), and Lagomarsino (1993). One of the recent trials to establish a reliable electronic damping database was made in Japan by collection of only high quality data from 285 buildings (Tamura et al., 2000) by a research committee of the Architectural Institute of Japan (AIJ). This committee conducted surveys on damping data from relatively new literatures and from 40 collaborative organizations.

Damping Predictors

Based on the AIJ Damping Database, Tamura et al. (2000) proposed the following damping predictors as empirical regression equations within the range of the tip drift ratio $x_H/H \leq 2\times10^{-5}$, for building heights in the range 10m<H<100m for RC buildings and 30m<H<200m for Steel buildings.

$$\zeta_1 = 0.014 f_1 + 470\frac{x_H}{H} - 0.0018 \qquad \text{: RC Buildings} \qquad (3)$$

$$\zeta_1 = 0.013 f_1 + 400\frac{x_H}{H} + 0.0029 \qquad \text{: Steel Buildings} \qquad (4)$$

Natural frequencies are also proposed as follows:

$$f_1 = \begin{cases} \dfrac{1}{0.015H} = \dfrac{67}{H} & \text{(For Habitability Level)} \quad (5a) \\ \dfrac{1}{0.018H} = \dfrac{56}{H} & \text{(For Safety Level)} \quad (5b) \end{cases} \qquad \text{: RC Buildings}$$

$$f_1 = \begin{cases} \dfrac{1}{0.020H} = \dfrac{50}{H} & \text{(For Habitability Level)} \quad (6a) \\ \dfrac{1}{0.024H} = \dfrac{42}{H} & \text{(For Safety Level)} \quad (6b) \end{cases} \qquad \text{:Steel Buildings}$$

It should be noted that the frequency dependent terms in Eqs.(3) and (4) are not actually the effect of the natural frequency. There is no clear reason for the frequency effects. They may be attributed to the effect of SSI. A low-rise building with a high natural frequency makes a significant contribution to the SSI effect. Thus, it tends to have higher total damping. Therefore, it is better to replace the frequency-dependent term with a height-dependent term as follows:

$$\zeta_1 = \frac{0.93}{H} + 470\frac{x_H}{H} - 0.0018 \qquad \text{: RC Buildings} \tag{7}$$

$$\zeta_1 = \frac{0.65}{H} + 400\frac{x_H}{H} + 0.0029 \qquad \text{: Steel Buildings} \tag{8}$$

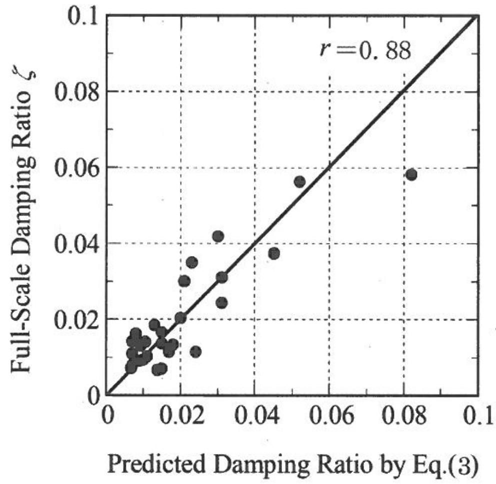

Figure 5 Comparison of known amplitude full-scale damping data with those predicted by Eq.(3) (Tamura et al., 2000)

The correlation coefficient of the damping values predicted by Eq.(3) and the full-scale values whose amplitudes are known, for example, was 88%, as shown in Fig.5. Thus, the predictors by Eqs.(3) and (4), or Eqs.(7) and (8) are believed to be very reliable.

Table 1 Design damping ratios for RC buildings

Building Height H (m)	Habitability			Safety (Elastic Range)		
	Natural Frequency (Hz) $f_1 = 1/0.015H$	Damping Ratio ζ_1 (%)		Natural Frequency (Hz) $f_1 = 1/0.018H$	Damping Ratio ζ_1 (%)	
		Rec.	Standard		Rec.	Standard
30	2.2	2.5	3	1.9	3	3.5
40	1.7	1.5	2	1.4	2	2.5
50	1.3	1.2	1.5	1.1	2	2.5
60	1.1	1.2	1.5	0.93	1.5	2
70	0.95	0.8	1	0.79	1.5	2
80	0.83	0.8	1	0.69	1.2	1.5
90	0.74	0.8	1	0.62	1.2	1.5
100	0.67	0.8	1	0.56	1.2	1.5

- "Rec." means "Recommended" values.
- The "Standard" values or larger values (max. ×1.2) can be used for buildings such as hotels and apartment houses, which have many interior walls.
- Less than the "Recommended" values should be used for buildings that have few interior walls.
- The value for H = 30m should be used for buildings lower than 30m.
- The tabulated values represent the damping ratios including SSI effects. Thus, they should not be used for structural damping of the upper structure.

Table 2 Design damping ratios for steel buildings

Building Height H (m)	Habitability			Safety (Elastic Range)		
	Natural Frequency (Hz) $f_1 = 1/0.020H$	Damping Ratio ζ_1 (%)		Natural Frequency (Hz) $f_1 = 1/0.024H$	Damping Ratio ζ_1 (%)	
		Rec.	Standard		Rec.	Standard
30	1.7	1.8	2.5	1.4	2	3
40	1.3	1.5	2	1.0	1.8	2.5
50	1.0	1	1.5	0.83	1.5	2
60	0.83	1	1.5	0.69	1.5	2
70	0.71	0.7	1	0.60	1.5	2
80	0.63	0.7	1	0.52	1	1.5
90	0.56	0.7	1	0.46	1	1.5
100	0.50	0.7	1	0.42	1	1.5
150	0.33	0.7	1	0.28	1	1.5
200	0.25	0.7	1	0.21	1	1.5

• The same notes as Table 1

Recommended Design Values of Structural Damping Ratio

Based on the proposed predictors and discussions on amplitude levels, Tamura et al. (2000) proposed to use the recommended values given in Tables 1 and 2 for designing RC buildings and steel buildings, respectively.

These damping ratios are for wind-induced response analyses for amplitude levels lower than the elastic limit of main frames under the assumption of no damage to secondary members and architectural finishing.

However, even in a very high amplitude range exceeding the elastic limit of the main frames, as the contribution of plastic-hysteretic damping becomes significant, it is recommended to use these values as the structural damping ratio.

DAMPING ESTIMATION TECHNIQUES

Modal identification techniques and damping estimation techniques are summarized in Tamura et al. (2005). Here, quality of estimated damping, points to note of damping estimation, and the efficiency of two user-friendly damping evaluation techniques are discussed.

Quality of Estimated Results

The dynamic characteristics of an actual full-scale structure can be obtained by traditional experimental modal analysis techniques. However, these techniques have the following limitations. Artificial excitation or input information is also necessary to measure the Frequency Response Functions (FRFs) or the Impulse Response Functions (IRFs) for subsequent modal parameter extraction. These response functions are very difficult to obtain under field conditions or for large structures. Some components, instead of the complete system, can be tested in the laboratory environment, but it is not easy to precisely simulate the boundary conditions.

Test procedures and estimation techniques significantly affect the quality of the obtained modal parameters, i.e. natural frequencies, damping ratios, and mode shapes. In order to obtain high quality estimates, it is necessary to conduct careful and high quality measurements. Especially in damping estimations, great care is required for high quality data acquisitions. In the building engineering field, chances to obtain full-scale measurements are quite rare, and obtained data are very valuable. Therefore, modal parameters obtained by full-scale measurements have been treated as a kind of precious heritage. This is true for natural frequencies and mode shapes obtained under field conditions, which have only 10% - 20% errors. However, low quality damping data can result in significant errors of 100% - 200% or more. Short term measurements at only a few points for Output-Only Modal Estimation (OOME) occasionally have almost no meaning in damping estimations and can provide nonsense results in some cases. Furthermore, it cannot be denied that many full-scale data have over-estimated damping ratios because of inappropriate measurements and damping estimation methods. Thus, it is very important to carefully examine the existing damping data and to have the courage to reject such contaminated damping data, even though almost no data would then be available.

Here, the efficiency of two simple and user-friendly but accurate damping estimation techniques is discussed. One is the Frequency Domain Decomposition (FDD) technique (Brincker et al., 2000) using Singular Value Decomposition (SVD) of the Power Spectral Density (PSD) matrix and the other is the Multi-mode Random Decrement (MRD) technique (Tamura et al., 2002). Both can be applied to ambient excitations such as wind, turbulence, traffic, and/or micro-tremors. Many civil engineering structures can be adequately excited by ambient excitations. Ambient modal analysis based on response measurements has two major advantages compared to traditional analysis. One is that no expensive and heavy excitation devices are required. The other is that all (or part) of the measurements can be used as references, and Multi-Input Multi-Output (MIMO) techniques can be used for modal analysis, thus enabling easy handling of closely-spaced and even repeated modes. This is most valuable for long-span roof structures or complex and huge systems such as power transmission line systems.

Points to Note in Damping Estimation

Measurements of a FDDR of a single-degree-of-freedom (SDOF) system can directly provide the system's Time Response Function (TRF). Here, TRF includes IRF, FDDR and the RD signature. The Logarithmic Decrement method (LD) is commonly used to give a quick estimate of the damping ratio from the TRF, represented by an exponentially decaying harmonic motion. Under field conditions, the FDDR signal is generally polluted by noise. More amplitude points are chosen and plotted on semi-logarithmic plane, and a straight line is obtained by linear regression. This technique is available for linear systems or structures. However, the dynamic properties of buildings generally have non-linearity, as shown in Fig.2. For actual buildings, the straight line approximation can only provide the average tendency; for accurate values, step-by-step estimation of the damping ratio for each amplitude level is necessary.

When dealing with a multiple-degree-of-freedom (MDOF) system, one can filter out the effect of other modes in the frequency domain and transform the signal back to the time domain. The accuracy of the method breaks down when there are two close modes.

In dynamic tests, where both input and output signals can be measured, FRF can be estimated by Auto PSD and Cross PSD through Fast Fourier Transform (FFT). The simplest technique for estimating damping ratios is the Half Power (HP) method directly using the Auto PSD of the responses. Actually, the bandwidth and the damping ratio can be more accurately evaluated from the imaginary or real part of FRF, the phase gradient, and the Nyquist plot in the complex plane.

It should be noted that damping estimation techniques in the frequency domain are more or less based on output PSDs, which require the following conditions for accurate estimation:

- stationarity of building responses
- sufficient frequency resolution near resonant frequency in FFT analysis

The first condition is closely related to the inherent nonlinearity of dynamic properties of buildings, shown in Figs.2, 3 and 4. Mixing of different levels of building responses results in a deformed or broader resonant peak providing inaccurate estimation of the damping ratio (Jeary, 1992).

The second condition comes from the leakage error in PSD estimation due to data truncation of Discrete Fourier Transform (DFT), which always takes place in practice. This generally results in a larger damping estimation, and occasionally it becomes very large. It has been emphasized by Jeary (1986), Tamura et al. (2002) and others, but there have been many papers reporting unrealistically large damping values without any consideration of this point. This is because natural frequencies and mode shapes are not significantly affected by insufficient frequency resolution.

Figure 6 demonstrates the importance of fine frequency resolution in damping estimation, say a sufficient length of sample or a sufficient number of DFT data points (Tamura et al., 2004). This is the result obtained from laboratory tests on ambient vibrations of a simple four-story lumped-mass model. Damping ratios were obtained by various frequency domain estimation methods, where the Auto PSDs or FRF was calculated via DFT. The abscissa indicates the number of data points used for DFT calculation. The evaluated damping ratios decrease with increasing number of DFT data points and converge to a constant value around 0.25%, which was thought to be the accurate damping value. If the number of DFTs were only set at 1024, as the fundamental estimation of PSD by FFT often does, the evaluated damping ratio can be 3%, which is more than 10 times the accurate damping value, thus producing a 1000% error. It is not appropriate to say "error" for a discrepancy of 100% or more: it should be called a "mistake".

Leakage is a kind of bias error that cannot be eliminated by windowing, e.g. by applying a Hanning window. Furthermore, it is harmful to the damping estimation accuracy, which relies on the PSD measurements. The bias error caused by leakage is proportional to the square of the frequency resolution (Bendat & Piersol, 1986). Therefore, increasing frequency resolution is a very effective way to reduce leakage error.

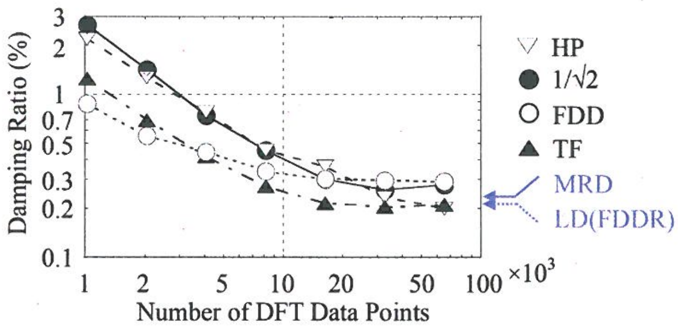

Figure 6 Variations of damping ratios evaluated by PSD-based frequency domain techniques with DFT data points demonstrating leakage effects

It is noted that the number of DFT data points should be more than 16,384 in this case, which is almost 600 times the natural period of the model, for accurate identification of the damping ratio. This means that the sample should have enough length. An ensemble averaging operation with a sufficient number of samples is also necessary to obtain a correct Auto PSD. A very long total record length is required to accurately evaluate the damping ratio by using a sufficient number of samples for ensemble averaging with enough length for each sample for fine frequency resolution. It is also noted that stationarity has to be satisfied in those records, which also requires careful selection of vibration records with similar conditions, especially in amplitude level.

Clearly, accurate damping can only be estimated by careful and time consuming efforts. As there is no theoretical means for estimating damping ratios in buildings, consulting high quality field data is the only way to make a good prediction of design damping value. It is thus necessary to establish a reliable database consisting of a statistically sufficient number of data sets of various structure types, building dimensions, architectural finishing, soil and foundation conditions, amplitudes and so on. It is necessary to accumulate a lot of high quality damping data.

Random Decrement (RD) Technique and Multi-mode Random Decrement (MRD) Technique

RD techniques for superimposing sub-samples of responses with an initial amplitude can be used to extract an Auto Correlation Function (ACF) eliminating randomly excited components (Cole, 1973, Jeary, 1986, Tamura & Suganuma, 1996). The RD technique assuming a SDOF system can efficiently evaluate the damping ratios and the natural frequencies only for well-separated vibration modes. It is very efficient for evaluating the amplitude dependency of the dynamic characteristics of buildings. However, if there are closely located predominant frequency components, a beating phenomenon is observed in the Random Decrement signature (RD signature). In these cases, traditional RD cannot be used to estimate the damping ratio. In order to evaluate multiple closely located vibration modes, the MRD technique has been proposed (Tamura et al., 2002), where the FDDRs of multiple SDOF systems with different dynamic characteristics are superimposed, and the least square (LS) curve fitting approximates the RD signature with the beating phenomenon.

The advantage of MRD is in application to closely located modes, which almost no traditional methods can do, and actual buildings and structures often have vibration modes that are not well-separated.

Frequency Domain Decomposition (FDD)

The FDD technique is a recently developed powerful tool that can be used in the frequency domain. Instead of using ASD of the building responses directly, as in the classical frequency domain technique, the PSD matrix is decomposed at each frequency line via SVD. SVD has a powerful property of separating noisy data from disturbance caused by unmodeled dynamics and measurement noise. For the analysis, Singular Value (SV) plots, as functions of frequencies, calculated from SVD can be used to determine modal frequencies and mode shapes. It has been proved that the peaks of an SV plot indicate the existence of structural modes (Brincker et al., 2000). The singular vector corresponding to the local maximum SV is unscaled mode shape. This is exactly true if the excitation process in the vicinity of the modal frequency is white noise. One of the major advantages of the FDD technique is that closely-spaced modes, even repeated modes, can be easily dealt with. The only approximation is that mode shape orthogonality is assumed.

The basic idea of the FDD technique is as follows (Brincker et al., 2001). The SV in the vicinity of the natural frequency is equivalent to the PSD function of the corresponding mode (as a SDOF system). This PSD function is identified around the peak by comparing the mode shape estimate with the singular vectors for the frequency lines around the peak. As long as a singular vector is found that has a high Modal Amplitude Coherence (MAC) value with the mode shape, the corresponding SV belongs to the SDOF function. If at a certain line none of the SVs has a singular vector with a MAC value larger than a certain limit value, the search for matching parts of the PSD function is terminated. From the fully or partially identified SDOF PSD function, the natural frequency and the damping ratio can be estimated by taking the PSD function back to the time domain by inverse FFT as an ACF of the SDOF system. From the ACF, the natural frequency and the damping are found by LD or other methods.

PRACTICAL APPLICATIONS OF MRD AND FDD TECHNIQUES

Application of MRD and FDD to Tall Chimney

Figure 7 shows an elevation and plan of the tested chimney, which consists of steel trusses and a concrete funnel, and has an octagonal cross section. Servo-type accelerometers were installed on three different levels. Two horizontal components (x, y) and one vertical component (z) were measured at each level. The sampling rate of the acceleration records was set at 100Hz, and ambient responses were measured for 90 minutes in total. Figure 8 shows the Auto PSD of acceleration (y-dir.) at the top of the chimney. Peaks corresponding to several natural frequencies are clearly shown. From such a beautifully isolated peak, it is generally easy to estimate the damping ratio, as well as the natural frequency, by the traditional RD technique.

The traditional RD technique assuming a SDOF system was applied for system identification using the ambient accelerations in the y direction at the top: GL+220m. By processing with a numerical band-pass filter with a frequency range of 0.06Hz - 1.0Hz, only the frequency components around the lowest peak near 0.4Hz depicted in Fig.8 were extracted. The initial amplitude of the acceleration to get the RD signature was set at the standard deviation. From the clear peak near 0.4Hz in the PSD shown in Fig.8, it was believed that the dynamic property of the first mode would be easily obtained with appropriate accuracy, but this was not correct. Figure 9 shows the obtained RD signature, where a beating phenomenon is observed, suggesting two closely located dominant frequency components. By careful examination of a close-up view of the peak near 0.4Hz, it is seen that there are actually two peaks: at 0.40Hz and 0.41Hz. It is very difficult to identify whether the peak at 0.41Hz seen in Fig.8 is meaningful or not from PSD due to FFT, and the traditional RD method based on SDOF fails to accurately estimate the damping ratio in such cases. However, the MRD technique can overcome this shortcoming of the traditional RD method.

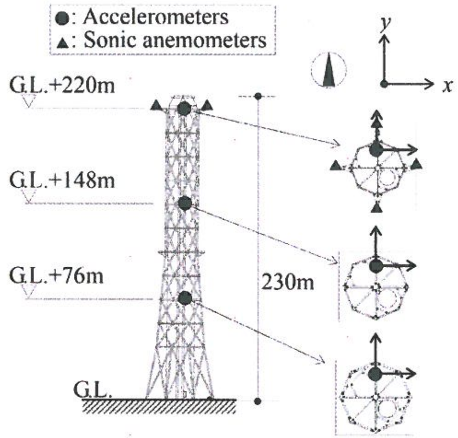

Figure 7 230m-high steel chimney

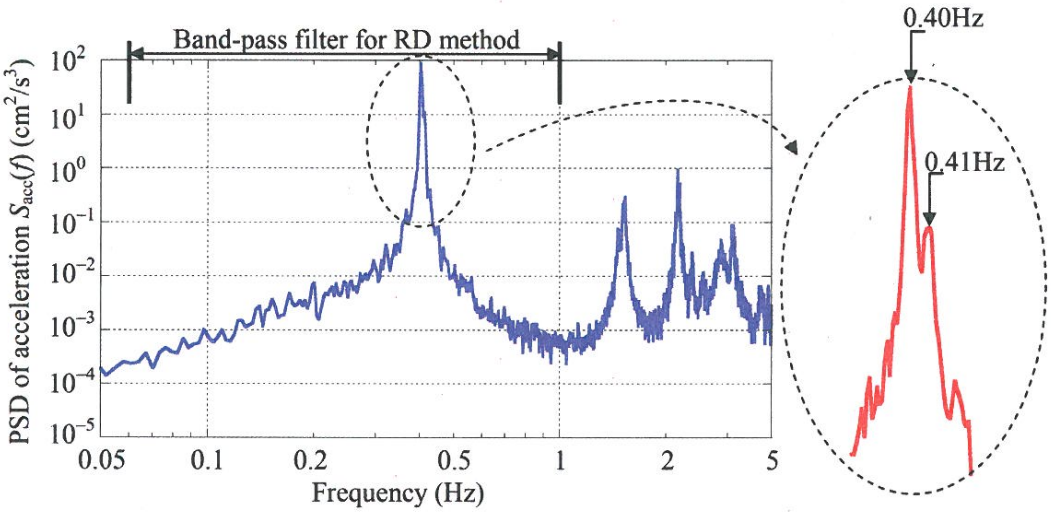

Figure 8 Auto PSD of tip acceleration (y dir.) of 230m-high chimney

The MRD technique (Tamura et al., 2002) was thus applied to approximate the beating RD signature, and the damping ratio and the natural frequency of the chimney were estimated at 0.18% and 0.40Hz for the 1st mode, and 0.30% and 0.41Hz for the 2nd mode, as shown in Fig.9. The dynamic characteristics of the 3rd and 4th modes were also estimated by the MRD technique.

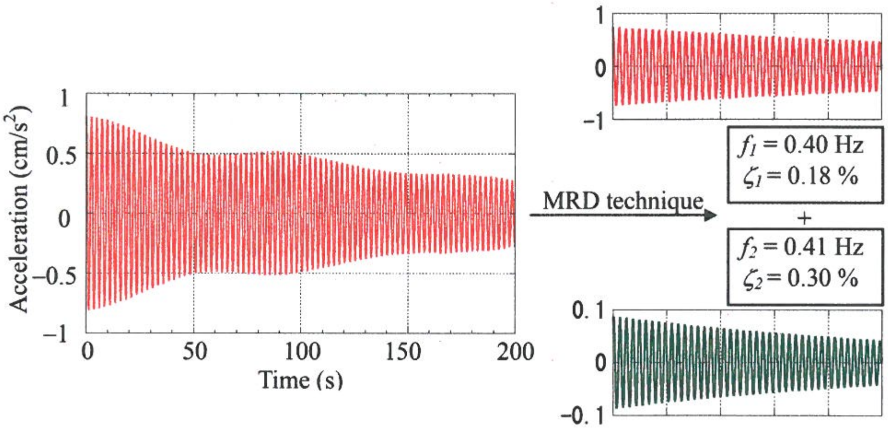

Figure 9 RD signature of tip acceleration (y-dir.) of 230m-high chimney and dynamic properties estimated by MRD technique

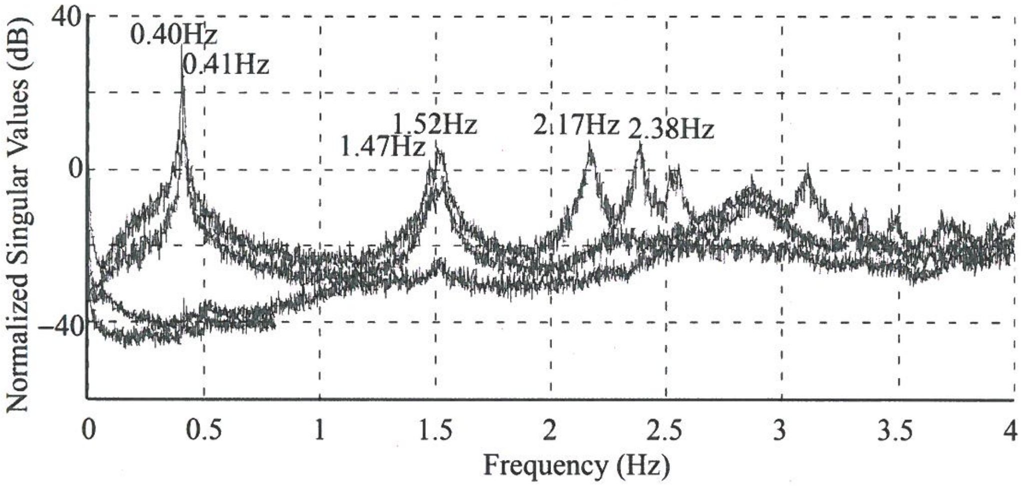

Figure 10 SV plots of 230m-high chimney

The FDD technique was also applied to the six horizontal components of the acceleration responses at the three different heights to evaluate the chimney's dynamic characteristics in detail. Figure 10 shows the frequency distribution of the SV plots obtained by the FDD technique from the PSD matrix of the acceleration responses. The 3rd and 4th natural frequencies are also closely located, and it is also very difficult to estimate damping ratios for these two modes by the HP method or the traditional RD technique. However, as shown, the FDD technique can estimate damping ratios even in such cases.

Figure 11 shows the damping ratios of the lowest two modes obtained by the FDD technique. The figure shows the effects of the number of data points used for PSD calculation on the estimated damping ratios. The damping ratios converge to certain values with increase in the number of data points, suggesting that it is necessary to take 8,192 data points in this case. Table 3 shows the dynamic characteristics of a 230m-high chimney obtained by MRD and FDD. They agree well except for the third mode damping ratio, and it is obvious that both techniques are useful even for closely located modes.

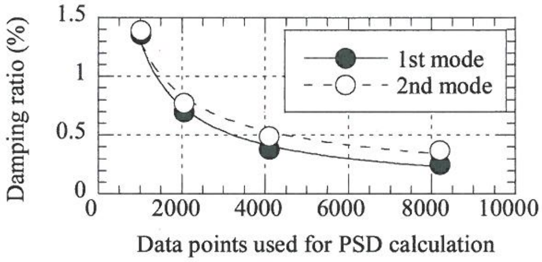

Figure 11 Variations of damping ratios of 230m-high chimney with DFT data points

Table 3 Dynamic characteristics of 230m-high chimney

Mode	Natural Frequency (Hz)		Damping Ratio (%)	
	MRD	FDD	MRD	FDD
1	0.40	0.40	0.18	0.24
2	0.41	0.41	0.30	0.39
3	1.47	1.47	0.83	0.3
4	1.53	1.52	0.85	0.91
5	2.17	2.17	0.55	0.65
6	2.38	2.38	0.42	0.39
7	-	2.87	-	-
8	-	3.10	-	0.77

Application of FDD to 15-story Office Building

A series of field measurements were made of ambient vibrations of a middle-rise 15-story office building, and its dynamic characteristics were evaluated (Tamura et al., 2002, and Miwa et al., 2002). The building extends from 6m underground to 59m above basement level, as shown in Fig.12. The columns are concrete-filled tube and the beams are wide-flange steel. The exterior walls of the first floor are of pre-cast concrete. The walls from the second floor to the top are of ALC. 14 servo-type accelerometers were used for one setup with two at the 15th floor as references, and 53 components were measured in total. By assuming that the floor was subject to lateral rigid body motion, the measured vibration was translated into equivalent motions at the desired corners.

The FDD technique was applied to evaluate the dynamic characteristics of the building based on the measured ambient vibrations. Cross spectral densities were estimated using the full data of 53 components.

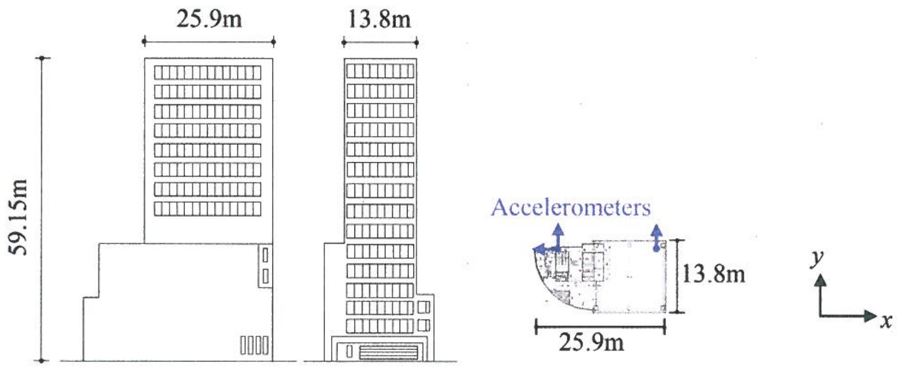

(a) Elevation (b) General plan

Figure 12 15-story office building

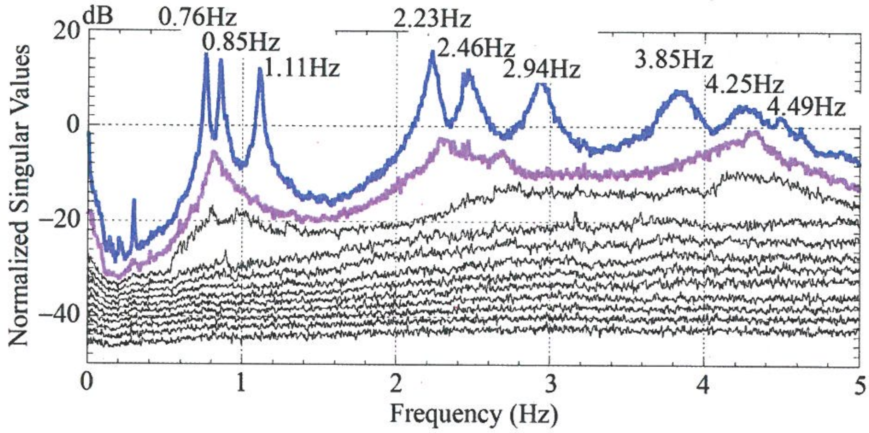

Figure 13 SV plots of 15-story office building

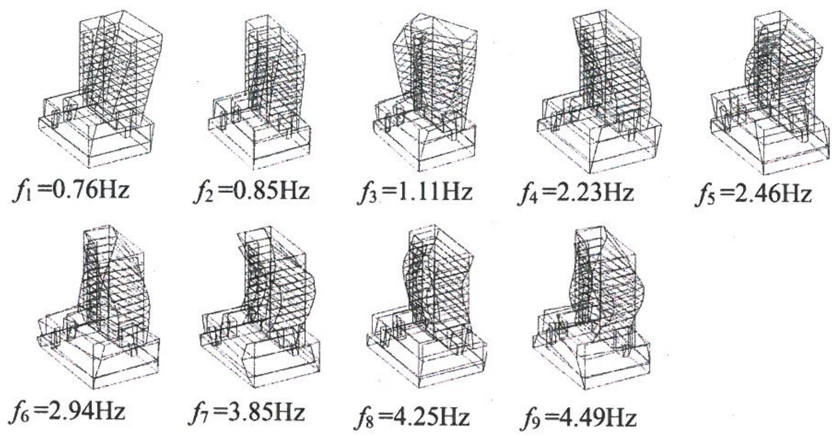

Figure 14 Mode shapes of 15-story office building obtained by FDD

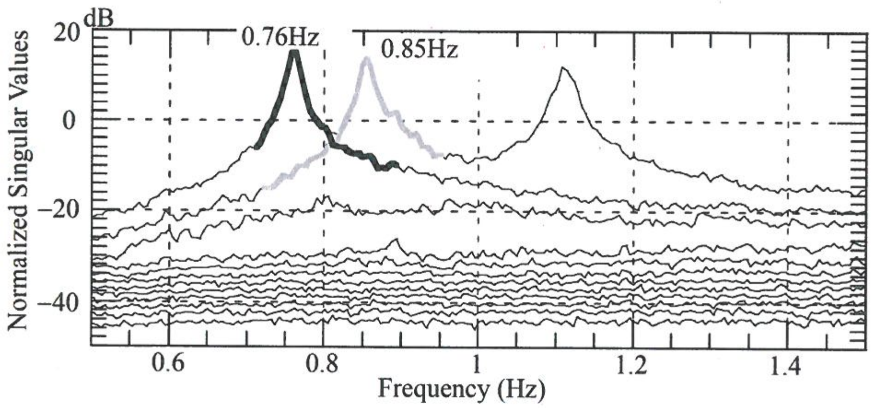

Figure 15 Close-up view of SV plots near the lowest mode of 15-story building

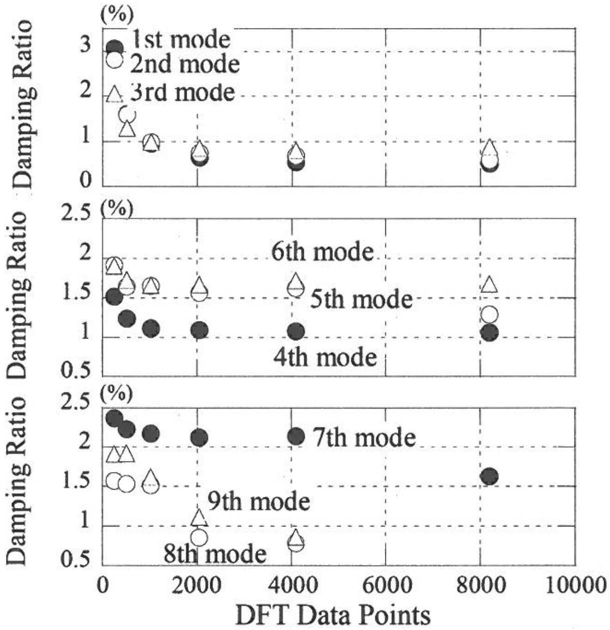

Figure 16 Variations of damping ratios of 15-story office building with DFT data points

Table 4 Dynamic characteristics of 15-story office building

Mode	Natural Frequency (Hz)			Damping Ratio (%)
	FEM Model	FDD (Full-scale)	Error(%)	FDD (Full-scale)
1	0.76	0.76	0	0.65
2	0.87	0.86	2.22	0.74
3	1.15	1.11	3.51	0.84
4	2.14	2.23	–3.99	1.10
5	2.53	2.47	2.59	1.56
6	3.02	2.94	2.82	1.67
7	3.85	3.85	0	2.12
8	4.26	4.26	0	0.85
9	4.67	4.47	4.29	1.11

Figure 13 shows the SV plots of the office building. There were many peaks of less than 5Hz corresponding to the natural frequencies, and it was possible to obtain up to the 9th mode below 5Hz. Figure 14 depicts the corresponding 9 mode shapes. Figure 15 shows a typical "bell" of the SDOF system: the 1st and 2nd modes of the 15-story building. From the identified SDOF spectral density function, the modal frequency and the damping can be estimated by taking the PSD function back to the time domain by inverse FFT as the ACF of the SDOF system. The modal frequency and the damping ratio are found from the ACF.

Figure 16 presents the variations of the damping ratios with the number of data points used for DFT calculation. The damping ratios of all modes decrease, while the number of data points, or frequency resolution, increases. It appears that damping estimates converge when the number of data points is large enough (up to 4096 or 8192).

Table 4 shows the dynamic characteristics of the 15-story building obtained by the FDD technique, where 4096 data points were used for DFT calculation. Corresponding natural frequencies obtained by FEM analysis are also shown in Table 4. In the original FEM analysis, the building's stiffness was estimated only for the members of the main structure, and the natural frequencies by FEM analysis were evaluated as slightly smaller than the full-scale values. The stiffness of the building's exterior walls was therefore added so that the first-mode natural frequency was identical to the full-scale value. As a result, satisfactory agreement with less than 5% error was obtained up to the 9th vibration mode, as shown in Table 4.

CONCLUDING REMARKS

The amplitude dependency of damping ratio was discussed, and the following facts were clarified. The critical tip drift ratio, at which damping ratio stops increasing with amplitude, was defined. The critical tip drift ratio was around $10^{-5} - 10^{-4}$. Damping ratio tends to decrease at higher amplitudes, unless there is no damage to secondary members and architectural finishing. Even for allowable stress level wind resistant design, the recommended damping ratio, e.g. that in AIJ2000, based on measurements rather low-amplitude regime should be used.

Various modal identification methods and damping estimation techniques were discussed, and the efficiency of two simple and user-friendly but accurate damping estimation techniques, MRD and FDD, were demonstrated. These two techniques are useful even where the natural frequencies are closely located, or even for repeated modes. It was also emphasized that a long period of measurements at a sufficient number of points is necessary to obtain high-quality damping data.

Insufficient measurements and inappropriate damping estimation methods can result in almost nonsense data, although the estimation of natural frequencies or mode shapes shows some robustness. As full-scale measurements are uncommon, field data are valuable. Therefore, contaminated damping data are all the more nuisances.

REFERENCES

Brincker, R., Zhang, L.M. and Anderson, P., 2000, Modal identification from ambient response using frequency domain decomposition, *Proceedings of the 18th International Modal Analysis Conference* (IMAC)

Brincker, R., Ventura, C.E. and Andersen, P., 2001, Damping estimation by frequency domain decomposition, *Proceedings of the 19th International Modal Analysis Conference* (IMAC)

Bendat, J. and Piersol, A., Random Data, 1986, Analysis and Measurement Procedures, *John 'Wiley & Son*, New York, USA, 1986

Cole, H. A., 1973, On-line failure detection and damping measurement of aerospace structures by the random decrement signatures, NASA CR-2205

Davenport, A.G. and Hill-Carroll, P., 1986, Damping in tall buildings: Its variability and treatment in design, Building Motion in Wind, *ASCE Spring Convention*, Seattle, 42-57

Fukuwa, N., Nishizawa, R., Yagi, S., Tanaka, K. and Tamura, Y., 1996, Field measurement of damping and natural frequency of an actual steel-framed building over a wide range of amplitude, *Journal of Wind Engineering and Industrial Aerodynamics*, **59**, 325-347

Haviland, R., 1976, A study of the uncertainties in the fundamental translational periods and damping values for real buildings, Massachusetts Institute of Technology, PB-253, 188

Jeary, A. P., 1986, Damping in buildings - a mechanism and a predictor, *Journal of Earthquake Engineering and Structural Dynamics*, **14**, 733-750

Jeary, A. P., 1992, Establishing non-linear damping characteristics of structures from non-stationary response time-histories, *The Structural Engineer*, **4**, **70**. 61-66

Lagomarsino, S., 1993, Forecast models for damping and vibration periods of buildings, *Journal of Wind Engineering and Industrial Aerodynamics*, **48**, 221-239

Miwa, M., Nakata, S., Tamura, Y., Fukushima, Y. and Otsuki, T., 2002, Modal identification by FEM analysis of a building with CFT columns, *Proceedings of the 20th International Modal Analysis*

Conference (IMAC)

Okada, K., Nakamura, Y., Shiba, K., Hayakawa, T., Tsuji, E., Ukita, T., Yamaura, N., 1993, Forced vibration tests of ORC200 Symbol Tower, Part 1 Test methods and results, Summaries of Technical Papers of Annual Meeting of Architectural Institute of Japan, Structures 1, 875-876

Tamura, Y. and Suganuma, S., 1996, Evaluation of amplitude-dependent damping and natural frequency of buildings during strong winds, *Journal of Wind Engineering and Industrial Aerodynamics*, **59**. 115-130

Tamura, Y., Suda, K. and Sasaki, A., 2000, Damping in buildings for wind resistant design, *Proceedings of the International Symposium on Wind and Structures for the 21st Century*, 26-28 January 2000, Cheju, Korea, 115-130

Tamura Y., Zhang L.-M., Yoshida A., Nakata S. and Itoh T., 2002, Ambient vibration tests and modal identification of structures by FDD and 2DOF-RD technique, *Structural Engineers World Congress (SEWC)*, Yokohama, Japan, October 9-12, T1-1-a-1, 8

Tamura, Y., Yoshida, A. and Zhang, L., 2004, Evaluation techniques for damping in buildings, *Wind Engineering & Science, International Workshop on Wind Engineering & Science*, October, 2004, New Delh

Tamura, Y., Yoshida, A. and Zhang, L., 2005, Damping in buildings and estimation techniques, *Proceedings of the Sixth Asia-Pacific Conference on Wind Engineering*, 12-14, September 2005, Seoul, Korea, CD-ROM

Wyatt, T.A., 1977, Mechanisms of damping, *Symposium on dynamic behaviour of bridges*, Transport and Road Research Laboratory, Crowthorne, Berkshire, 19 May 1977